Oxygen vacancy filament formation in TiO_2: A kinetic Monte Carlo study

Duo Li,[1] Maozhi Li,[2] Ferdows Zahid,[1] Jian Wang,[1] and Hong Guo[1,3]
[1]*Department of Physics and the Center of Theoretical and Computational Physics, The University of Hong Kong, Hong Kong*
[2]*Department of Physics, Renmin University of China, Beijing 100872 China*
[3]*Center for the Physics of Materials and Department of Physics, McGill University, Montreal, PQ H3A 2T8, Canada*

(Received 30 July 2012; accepted 5 September 2012; published online 5 October 2012)

We report a kinetic Monte Carlo (kMC) investigation of an atomistic model for 3-dimensional structural configurations of TiO_2 memristor, focusing on the oxygen vacancy migration and interaction under an external voltage bias. kMC allows the access of experimental time scales so that the formation of well defined vacancy filaments in thin TiO_2 films can be simulated. The results show that the electric field drives vacancy migration; and vacancy hopping-induced localized electric field plays a key role for the filament evolution. Using the kMC structure of the filaments at different stages of the formation process, electronic density of states (DOS) are calculated by density functional theory. Filament induced gap states are found which gives rise to a transition from insulating behavior to conducting behavior during the filament formation process. By varying kMC simulations parameters, relations between vacancy diffusion, filament formation, and DOS in the TiO_2 thin film are elucidated. © *2012 American Institute of Physics*.
[http://dx.doi.org/10.1063/1.4757584]

I. INTRODUCTION

The development of future information technology requires faster, denser, and less energy-consuming memory devices than what is available today. In this regard, the resistive switching random access memory (RRAM) has been one of the most exciting new candidates for terabit non-volatile memory due to its fast switching time, low energy requirement, high scalability, and long durability. For these reasons, RRAM has been investigated intensively.[1–3] Generally speaking, RRAM is operated between two phases of materials having different resistances. The phases with high or low values of resistance code the digital information. Writing information into RRAM induces a resistance switching. So far, $SrTiO_3$, $Ge_2Sb_2Te_5$, and TiO_2 and so on have been characterized as promising candidates for fabricating RRAM devices, among which TiO_2 has been paid particular attention,[4–8] since it has been characterized as a memristor[9]—a concept which conjectured non-linear circuit element relating charge and magnetic flux discussed in Chua's seminal paper of 1971.[10,11] In practice, a memristor can be considered as a device having the property that its resistance increases or decreases depending on the direction of the external voltage bias. Recently, intensive studies have shown that the migration of oxygen vacancies in TiO_2 under an applied voltage bias plays an important role of the resistance switching. Experiments have demonstrated that the formation of localized vacancy filaments in the conductive phase, known as Magnéli, is likely responsible for the resistance switching.[12,13] Specifically, the vacancy migration was characterized as a pipe diffusion,[14] under external voltage bias, acting as dopants and permitting the formation of 1-dimensional (1D) filamentary conducting channels in TiO_2 memristor. Once the filaments bridge the two electrodes, the resistance of the system is reduced. When external bias voltage is reversed, the filaments retract and the conducting channel is cut off, leading to a high resistance. While this resistance switching mechanism is plausible and consistent with certain experimental data, some other experimental evidence showed that the resistance switching may also come from electrochemical processes involving oxygen vacancies happening at the oxide-metal interface in the RRAM device.[15] Therefore, although experiments have shown clear relation between oxygen vacancies and resistance switching, the detailed switching mechanism is still unclear.

Meanwhile, some theoretical models were proposed for the understanding of the resistance switching mechanism, the forming stage characteristics of the electrochemical reaction, and the formation of the oxygen-vacancy in memristors.[8,16,17] In terms of electrochemical reactions involving oxygen ions/vacancies at the interface between electrodes and electrolyte, the switching behavior in a $Pt/TiO_2/Pt$ resistive switching cell was studied.[16] The applied voltage varies the oxygen-vacancy density at the interface, leading to the change of Schottky barrier height at the interface and consequently giving rise to a resistive switching.[16] However, the effect of the vacancy migration or configuration on the switching mechanism was not investigated in details. Moreover, since 3D structural configurations of the TiO_{2-x} phase in TiO_2 were not taken into account, some critical issues for the reality of RRAM devices such as switching speed and endurance cannot be addressed in this model. A continuum model taking into account the nonlinear dopant kinetics was proposed for the switching mechanisms and current-voltage characteristics.[17] However, it cannot provide an atomistic picture for the resistive switching mechanisms. On the other hand, molecular dynamics simulations were performed for the kinetic behavior of oxygen vacancies in oxide

 © 2012 American Institute of Physics

Downloaded 07 May 2013 to 147.8.230.100. This article is copyrighted as indicated in the abstract. Reuse of AIP content is subject to the terms at: http://jap.aip.org/about/rights_and_permissions

memristors interacting via realistic potentials and driven by an electric field, and various vacancy configurations were obtained. However, it fails to reproduce the localized conductive filaments, but only a uniform distribution model.[8] In addition, the time scale in molecular dynamics simulation is much shorter than that in experiments. Therefore, various factors affect the resistance switching mechanism in TiO_2 memristor, such as the electrochemical reactions at the interface, the oxygen-vacancy density at the interface, the vacancy migration, and the vacancy configuration in TiO_2, which makes a complete understanding of the switching mechanism in memristors quite difficult. In this work, we will focus on the effect of vacancy migration and configuration on the switching mechanism in realistic memristor materials at atomic level.

In particular, we developed an atomistic model with realistic 3D structural configuration to investigate vacancy diffusion and interaction under an applied bias voltage, and provide an atomic understanding into the mechanism of the filament configuration formation and electronic feature in the TiO_2 memristor material for the development of future RRAM. A kinetic Monte Carlo (kMC) simulation approach is implemented to investigate the vacancy structures and morphologies under various conditions at the electroforming stage. kMC is advantageous for this stage because it allows the access of experimental time scales for models at the atomic level. Well-defined vacancy filamentary channels are obtained in the kMC simulation. The vacancy migration is driven by the electric field and the vacancy hopping induces localized electric fields in TiO_2 which further enhance the local hopping rates, leading to the eventual formation of the vacancy filaments. Based on the kMC simulated filaments at different times, density functional theory (DFT) calculations reveal the emergence of defect states at the Fermi level as the filament is forming under bias voltage. These filament induced gap states clearly indicate an insulator to conductor transition. Our results give rise to an explicit atomistic mechanism of filament formation in TiO_2 thin films and its relation to the resistance switching phenomenon.

In Sec. II, the details of our kMC modeling for the oxygen vacancy filament formation are described. The kMC simulation results and related discussion are presented in Sec. III. The effect of vacancy filament configuration on the electronic density of states (DOS) is investigated in Sec. IV. Finally, a conclusion is given in Sec. V.

II. KINETIC MONTE CARLO MODELING

In our model, a system of TiO_2 thin film with two metal contacts at each side is considered as shown in Fig. 1(a). The two metal contacts serve as the electrodes for an applied bias voltage. For TiO_2 thin film, a crystal structure in the rutile phase is considered as it is the most stable phase and can be obtained experimentally.[13,18] Fig. 1(b) shows the primitive unit cell of the rutile phase, in which grey and red balls denote titanium (Ti) and oxygen (O) atoms, respectively. Once oxygen vacancies are present in TiO_2 thin film, these mobile charges hop in thin film under applied voltage. In our model, the oxygen vacancies can only hop between the nearest oxygen sites. Since we are interested in the vacancy configuration in TiO_2 thin film, the detailed structure of metal contacts is not considered. Three major vacancy diffusion processes are illustrated in Fig. 1(a), including vacancy diffusion in the TiO_2 thin film; diffusion along the interfaces between anode and TiO_2 thin film; and vacancy detachment from the interface. The corresponding activation energy barriers without voltage bias are denoted as E_0, E_{int}, and E_{det}, respectively. These processes are fundamental and indispensable for this memristive material.[19] Without bias voltage, the vacancy hopping rate can be evaluated as $D_h = D_0 \exp[-(E/(k_B T)]$, where E represents E_0, E_{int}, or E_{det}, k_B is the Boltzmman constant and T is the temperature. D_0 is the attempt frequency which we fix to a typical value of atomistic processes, $1.0 \times 10^{12}/\mathrm{s}$. In this work, we fix $E_0 = 1.1\,\mathrm{eV}$ according to the experimental estimate of the intrinsic diffusion of bridge-bonded vacancies.[21] Such high activation energy indicates that the hopping rate of single vacancies is very small at room temperature without bias voltage and may explain the experimental observation[22] that resistance of old samples could persist for months without significance change. It is also worth noting that a high activation energy of vacancy diffusion in TiO_2 is a desired property to achieve both high switching speed ($<100\,\mathrm{ns}$) and long retention time (>10 yr).[24] Activation energy barriers E_{det} and E_{int} are more difficult to estimate, so that we treat them as free parameters with initial values to be $1.1\mathrm{eV}(=E_0)$ and $0.7\,\mathrm{eV}$, respectively.

When a voltage bias is applied along the (001) or z direction,[20] the potential energy surface will be modified and the energy barrier will be lowered along this direction, thereby inducing vacancy hopping. As a result, vacancy hopping is now determined by a modified time t dependent

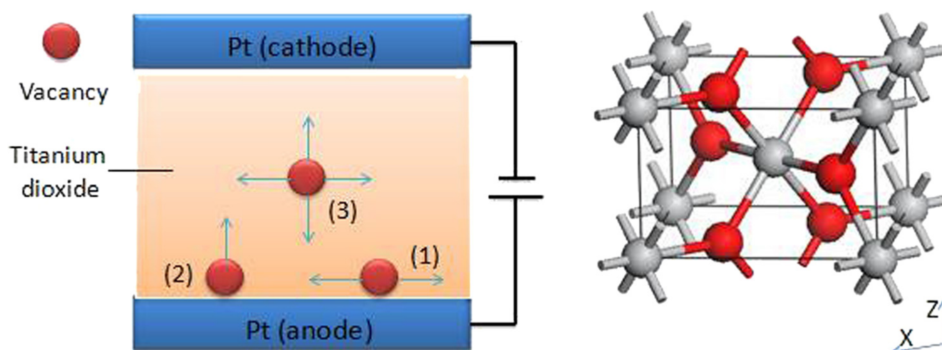

FIG. 1. (a) Schamtic of the system of the TiO_2 thin film and two metal electrodes. Illustration of three major vacancy diffusion processes in our model: vacancy diffusion in bulk TiO_2 (3), interface diffusion (1), and vacancy detachment from interface (2). (b) Primitive unit cell of TiO_2 for the rutile phase. Grey and red balls represent Ti and O atoms, respectively.

Downloaded 07 May 2013 to 147.8.230.100. This article is copyrighted as indicated in the abstract. Reuse of AIP content is subject to the terms at: http://jap.aip.org/about/rights_and_permissions

hopping rate, $D_z(t) = D_0 \exp[-(E - E_{bias}(t))/(k_B T)]$, where $E_{bias}(t)$ is the reduced energy barrier caused by the applied bias voltage. It is time dependent because the voltage bias is changing with time. For applied voltage bias, the experimental scenario is considered, where the electroforming process is driven by $V(t) = \lambda \times t$ in the first half period and $V(t) = V_{max} - \lambda \times t$ in the second half period. Here λ is the voltage sweeping rate and V_{max} is the maximum voltage bias. $V_{max} = 1\text{V}$ was chosen according to the experiments,[25] and a sweeping rate of $\lambda = 0.02\,\text{V/s}$ is used in our simulations. For the capacitor-like geometry of Fig. 1(a) under voltage bias, the reduced energy barrier E_{bias}(t) for vacancy hopping can be assumed to depend linearly on voltage bias as $E_{bias}(t) = \alpha V(t)$, where the coefficient α typically has values of $0.4 \sim 0.5\,\text{eV/V}$.[23] Here, we fixed $\alpha = 0.4\,\text{eV/V}$ which makes the corresponding energy barriers of vacancy hopping along z direction comparable to E_{int} as voltage reaches the maximum value.

Since the vacancies are mobile charges, the Coulomb repulsions between vacancies are also considered when the vacancies are within the nearest neighbor distance. Coulomb repulsion helps to lower the energy barrier for the selected vacancy to hop to the target sites. The reduced energy barrier caused by Coulomb repulsion is denoted by E_c. Physically, it is reasonable to assume that the Coulomb interaction is proportional to the number of the nearest neighbor vacancies, so that $E_c = \beta N$ where β is the reduced energy barrier caused by the interaction between two nearest vacancies. Considering the large dielectric constant of TiO_2, a reasonable value of $\beta = 0.1\,\text{eV}$ is used throughout the kMC simulation. In our model, the temperature distribution within the system is assumed to be uniform. This is reasonable because experimentally the I-V curve is not sensitive to temperature in a wide range ($200 \sim 305\,\text{K}$).[13] It was also known that simple thermal effect was not enough to generate the observed resistance switching phenomenon.[26] Therefore, we may focus on the local electric field which appears to have the most important effect on vacancy evolution.[27]

In our kMC simulation, an TiO_2 thin film of $15 \times 30 \times 10$ unit cells with 300 vacancies populated at the metal-TiO_2 interface of the anode is incorporated to be the initial configuration as shown in Fig. 2. This choice of the vacancy population at the interface is motivated by the experiments,[15] where heavy vacancies were doped at the interface. On the other hand, even without doping at the interface, thermal diffusion of metal atoms in adhesion layers through the electrode layer also leads to a significant vacancy population at the interface.[28] Therefore, 300 vacancies are initially populated at the interface of anode. For the thickness of TiO_2 thin film, it is limited within 3 nm (roughly 10 lattice constants) in our model, since we focus on the filament formation. This is justified as experiments showed that two mechanisms, filamentary and homogeneous switching patterns, may be responsible for the resistance switching. For the filamentary switching pattern, a typical length scale of filament is about $3 \sim 5$nm. Above 5 nm, before conductance channel is formed, more vacancies will populate in TiO_2 thin film, so that homogeneous switching pattern will be formed and coexist with filamentary switching pattern.[29]

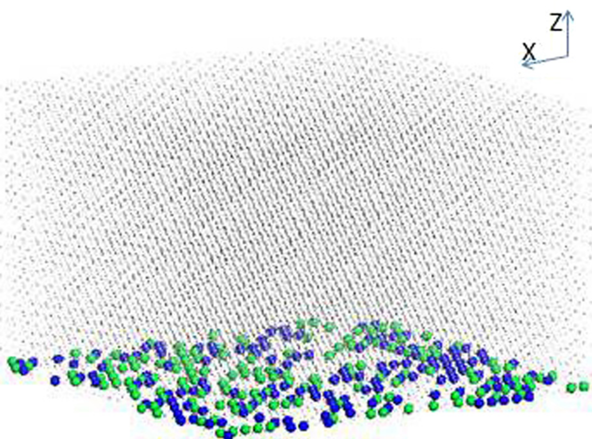

FIG. 2. Initial configuration of TiO_2 thin film of $15 \times 30 \times 10$ unit cells with 300 vacancies doped at the interface between thin film and anode. The electrodes are not presented.

III. VACANCY FILAMENT FORMATION

We performed kMC simulations for the initial configuration shown in Fig. 2 to investigate the effect of electric field, voltage sweep rate, and energy barriers on the vacancy filament formation under voltage bias.

A. Electric field

First, we assume that the electric field in the TiO_2 film was distributed uniformly. As a result, the modified vacancy hopping rate caused by the applied voltage bias is the same for all the vacancies populating at the interface of thin film and anode, so that all the vacancies will simultaneously hop into the film in the entire electroforming process. It is expected that the simulation produces a homogeneous distribution of vacancies in TiO_{2-x} thin film, which will lead to the so-called homogeneous switching pattern as mentioned above. Apparently, the simulated vacancy configuration is not consistent with experiments[29] where within 3 nm thick thin film, filamentary switching pattern should dominate.

Since vacancies are charged objects, assuming an uniform electric field is too simple. It is more reasonable to assume that the electric field is uniform before any vacancies hop into the TiO_2 thin film. However, once a vacancy hops into the thin film, the electric field surrounding this vacancy site is enhanced.[27] Consequently, other vacancies diffusing along the interface and arriving near this vacancy site are driven by the locally enhanced electric field and hop into the film, leading to a diffusion channel of the vacancies. Based on the above assumption, we performed kMC simulations in the case of non-uniform electric field.

Figure 3 shows four representative configurations at different voltages in an electroforming switch period obtained from kMC simulations in the non-uniform field case. As shown, no vacancy detaches from the interface of thin film and anode as voltage is increased to 0.5 V. When $V = 1.0\,\text{V}$, some vacancies are observed in the central region of the device. As V is swept back to 0.5 V, more vacancies keep hopping into the central region as shown in Fig. 3(c). Finally, a

Downloaded 07 May 2013 to 147.8.230.100. This article is copyrighted as indicated in the abstract. Reuse of AIP content is subject to the terms at: http://jap.aip.org/about/rights_and_permissions

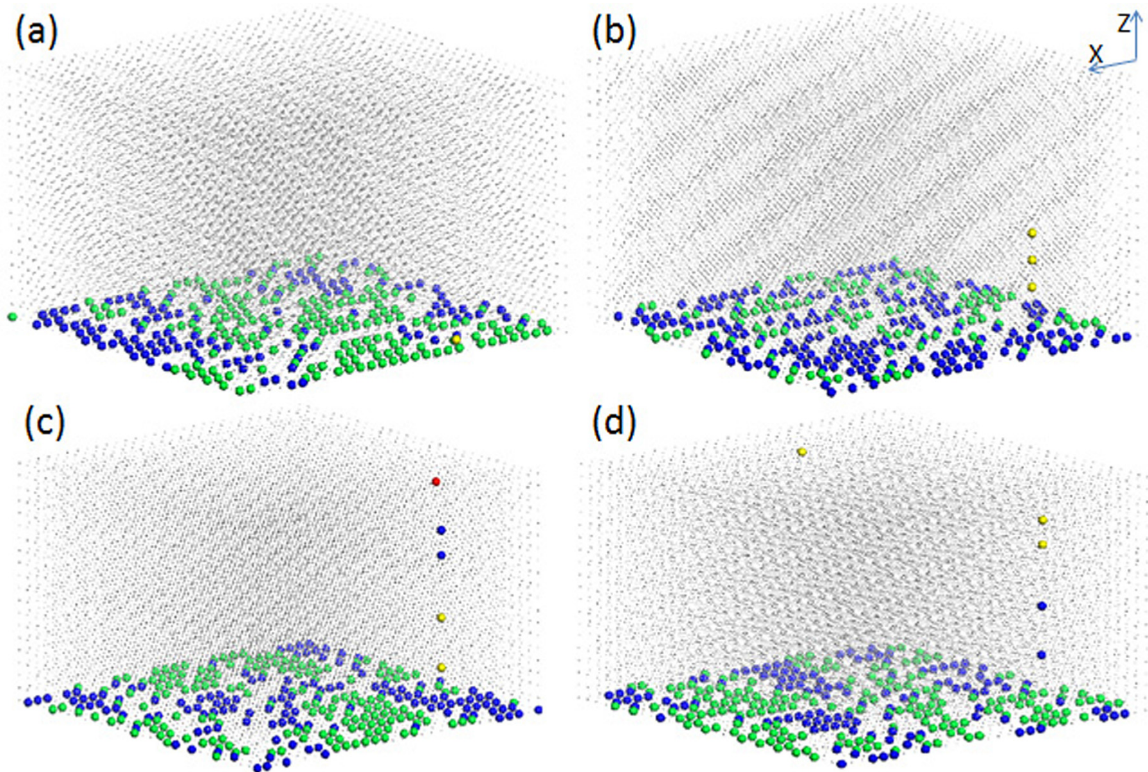

FIG. 3. Representative configurations at (a) $t = 25$ s, $V = 0.5$ V; (b) $t = 50$ s, $V_{max} = 1.0$ V; (c) $t = 75$ s, $V = 0.5$ V; (d) $t = 100$ s, $V = 0$ V. Here $E_{det} = 1.1$ eV, $E_{int} = 0.7$ eV, $\lambda = 0.02$ V/s.

vacancy filament is formed in bulk TiO_2. The simulated configuration shown in Fig. 3 is in good agreement with previous study.[30] As shown in Fig. 3(d), there is one filament formed and its resistance switching can be easily predicted which is crucial for the stability of the device at initial stage. If multiple parallel filaments are formed, the hysteresis loop would become twisted.[31]

As observed in Fig. 3(d), for the energy barriers and parameters, we investigated 4–5 vacancies can detach from the interface hop into TiO_2, and form a filament channel. In the simulated structure configurations, the TiO_2 film thickness is around 3 nm—roughly 10 unit cells. The statistical analysis for several simulated configurations shows that every two unit cells contain one oxygen-vacancy in the filamentary channel. This is quantitatively consistent with the Magnéli phase of Ti_4O_7 observed in experiments,[13] which also indicates that our parameters used in the kMC simulations are physically reasonable.

B. Forming time and threshold voltage

One particular issue in device physics is the switching time, i.e., the so called "voltage-time" dilemma.[32] Even though a conducting channel will be eventually formed no matter how slow a voltage is swept, the time scale of the electroforming process can be significantly different. To this end, we monitored the voltage (called threshold voltage) and time needed for the first vacancy to arrive at the top electrode, for various sweep rates λ. Clearly, when the first vacancy arrives, there are some other vacancies populating in the TiO_2 film. As shown in Fig. 4, the forming time changes significantly if the sweep rate is small. When sweep rate is larger than 0.02 V/s, the change of forming time significantly slows down. In contrast to forming times, the threshold voltage does not change significantly with the sweep rate. This is partly due to the high activation energy for bulk diffusion, which makes the vacancy migration have very small probability unless the threshold voltage is achieved. In addition, this also depends on the film thickness as demonstrated in experiment.[32] Fig. 4 also shows the effect of coefficient α on the forming time and threshold voltage. A larger α reduces the energy barriers thereby lowers the threshold voltage and shortens the filament forming time. Nevertheless, the effect

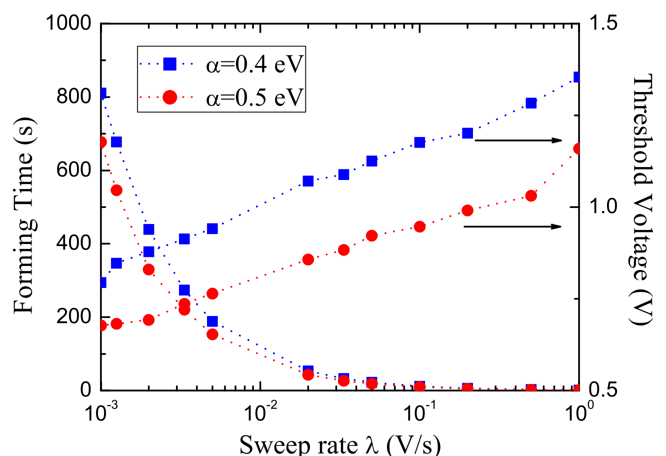

FIG. 4. The dependence of simulated forming time and threshold voltage on sweep rate. The circle and square symbols are for $\alpha = 0.4$ eV and 0.5 eV, respectively.

Downloaded 07 May 2013 to 147.8.230.100. This article is copyrighted as indicated in the abstract. Reuse of AIP content is subject to the terms at: http://jap.aip.org/about/rights_and_permissions

of α on forming time becomes weaker as the sweep rate increases. The effect of α on the threshold voltage does not change significantly with the sweep rate.

As shown in Fig. 4, the threshold voltage changes logarithmically with sweeping rate λ. This behavior is quite similar to that of the switching time dependence of threshold voltage observed in $Ge_2Sb_2Te_5$,[33] a chalcogenide phase change memory (PCM) material where the resistance switching is facilitated by the reversible amorphous-to crystalline phase changes triggered by bias voltage. Although PCM and memristors are two different classes of materials for fabricating RRAM devices, the behavior of threshold voltage with switching time is similar. This may imply that the switching mechanism in these two systems may share a certain common feature.

The effect of vacancy detachment from interface can be investigated by varying the value of E_{det}. Fig. 5 shows the typical configurations under different voltages with $E_{det} = 1.0\,\text{eV}$ (instead of 1.1 eV as studied above). The smaller the detachment energy barrier, the more vacancies hop into the central region. Statistically, there can be eight or nine vacancies in the channel (3 nm length) under the maximum voltage, which is significantly more than that in the case of $E_{det} = 1.1\,\text{eV}$. Furthermore, several parallel filaments are formed. This indicates that smaller values of E_{det} may lead to the situation where homogeneous switching pattern dominates. We also investigated the effect of vacancy diffusion along the metal-TiO_2 interface which is detrimental to the filament formation. Our detailed analysis shows that as long as $E_{int} \sim 0.7\,\text{eV}$ or larger, reasonable vacancy filamentary configurations can be formed to bridge the two metal contacts.

IV. ELECTRONIC DENSITY OF STATES

The formation of vacancy filaments bridging the two metal contacts should have substantial influence on the electronic and charge transport properties of the memristor. To this end, we have calculated the DOS of the system using the atomic first principles methods as implemented in the state-of-the-art quantum transport package NanoDcal.[34] Nanodcal implements DFT within the Keldysh nonequilibrium Green's function (NEGF) formalism whose theoretical background can be found elsewhere.[35] To calculate the density of states at equilibrium, the NEGF-DFT formalism reduces to the standard DFT. In our calculations, a double-zeta polarized atomic orbital basis set is used to expand the wave functions and physical quantities, the exchange-correlation is treated at the local density approximation level,[36] and the atomic cores are defined by a nonlocal norm conserving pseudopotential.[37] A supercell of $1 \times 1 \times 10$ was employed (containing 20 Ti and 40 oxygen atoms), which represents a typical filament obtained in our kMC simulations. For k-sampling, $9 \times 9 \times 1$ and $11 \times 11 \times 3$ meshes are used for bulk pristine rutile and vacancy doped structures, respectively. The relaxed atomic positions are directly extracted from experiments. The error tolerance of self-consistency DFT iteration is set at 10^{-4}eV. As shown in Fig. 3, one oxygen is removed in every two unit cells each time, and a maximum of five oxygen vacancies can exist in a filament.

Figure 6 plots the DOS in a filament configuration with different vacancy numbers, consistent with previous results.[6] Without vacancy, the pristine rutile structure is an insulator with a wide band gap (blue line). However, as the vacancy number increases, defect states inside the original band gap

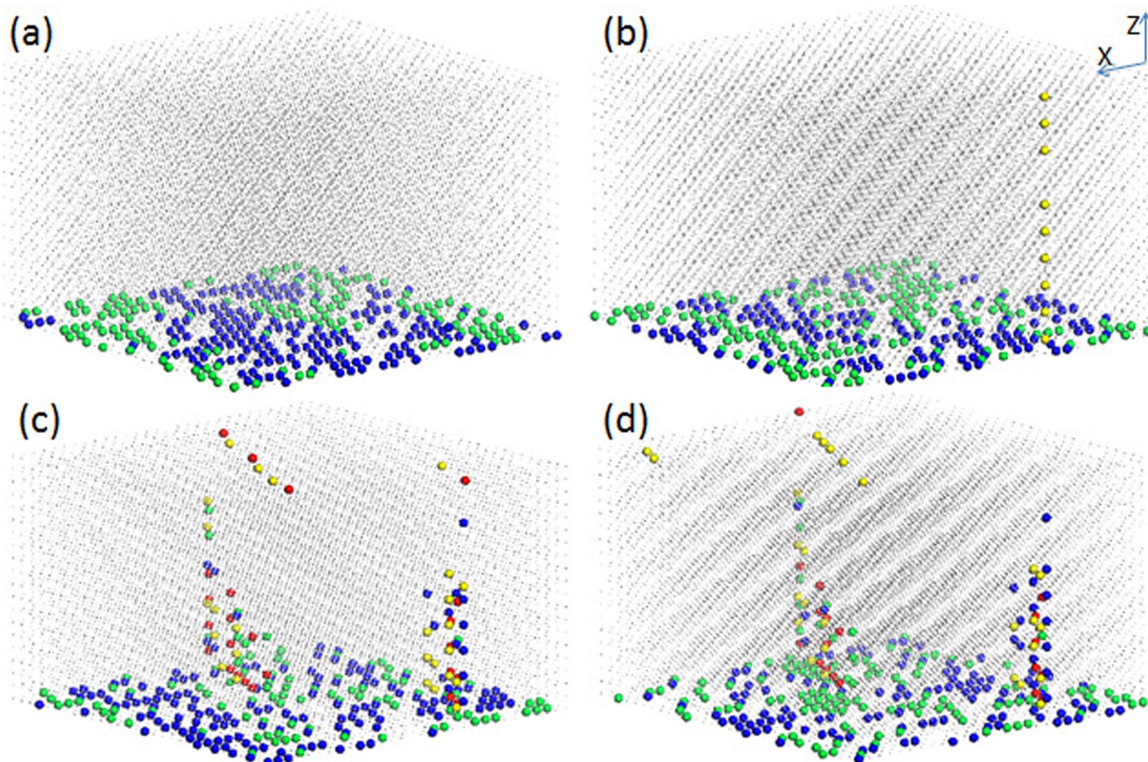

FIG. 5. Representative configurations with the choice of $E_{det} = 1.0\,\text{eV}$, $E_{int} = 0.7\,\text{eV}$, $\lambda = 0.02\,\text{V/s}$. (a) $t = 25\,\text{s}$, $V = 0.5\,\text{V}$; (b) $t = 50\,\text{s}$, $V_{max} = 1.0\,\text{V}$; (c) $t = 75\,\text{s}$, $V = 0.5\,\text{V}$; (d) $t = 100\,\text{s}$, $V = 0\,\text{V}$.

Downloaded 07 May 2013 to 147.8.230.100. This article is copyrighted as indicated in the abstract. Reuse of AIP content is subject to the terms at: http://jap.aip.org/about/rights_and_permissions

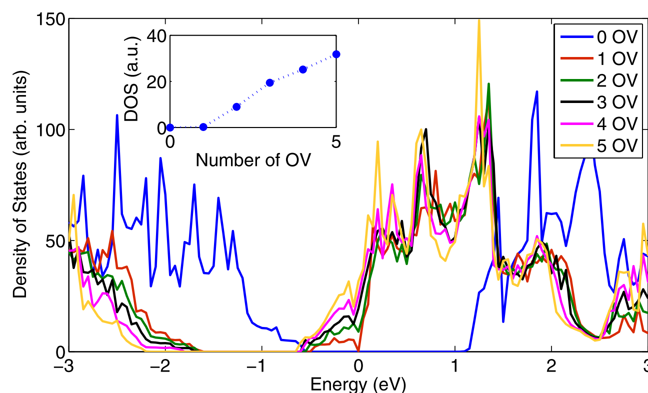

FIG. 6. Density of states with various numbers of oxygen vacancies. The Fermi levels are shifted to 0 eV. Inset: states vs vacancy numbers at the Fermi level.

at the Fermi energy (energy zero in Fig. 6) emerge and become more pronounced. The vacancy filament therefore induces gap states that turn the material into a conducting state. Clearly, if the external bias is reversed, the vacancies in the filament will retract because the hopping rate in the $-\mathbf{z}$ direction is now lowered. This way, the resistance is small or large depending on the polarity of the external bias. For the 3 nm thin TiO_2 film, the inset in Fig. 6 shows that the DOS increases dramatically where there are two vacancies in the filament, afterward it increases almost linearly with the vacancy number. This suggests that although there are vacancy defects at the metal-TiO_2 interface during material growth, the memristor behaves as an insulator at the beginning of the voltage cycle.

Finally, note that broad DOS features appear in the band gap when vacancies are introduced in the supercell. This is due to broadening of the vacancy levels when the vacancy interacts with other atoms in the supercell. A small additional broadening may be due to the finite size effect of the supercell. Qualitatively and most importantly, the change of DOS against the concentration of oxygen vacancy is quite clear and the appearance of gap DOS indicates a change of transport from that of a wide-band insulator to a conductor.

V. CONCLUSION

We have implemented a simple but effective kMC approach to investigate the oxygen vacancy filament formation process in 3-dimensional TiO_2 memristor structures. kMC allows the access of experimental time scales so that the formation of well defined vacancy filaments in thin TiO_2 films can be simulated at the atomic level. The results show that the electric field drives vacancy migration from one electrode contact to the other, and in the process, the vacancy hopping-induced localized electric field plays a key role. Using the kMC structure of the filaments at different times, electronic density of states are calculated by density functional theory. Filament induced gap states are found which gives rise to significant DOS at the Fermi level when there are even only two vacancies in a TiO_2 channel of 3 nm long. The DOS increases roughly linearly as more vacancies are injected by the external bias. The gap states gives rise to a transition from insulating behavior to conducting behavior. By varying kMC simulations parameters, relations between vacancy diffusion, filament formation, and DOS in the TiO_2 thin film is elucidated; in particular, the filament formation and electric properties of TiO_2 thin films are very closely related.

ACKNOWLEDGMENTS

The authors thank B. Wang and L. Zhang for discussions on the DFT method. We are grateful to Research Grant Council (HKU 705611 P) and University Grant Council (Contract No. AoE/P-04/08) of the Government of HKSAR (J.W. and F.Z.); National Basic Research Program of China (No. 2012CB932704), NSFC (51071174), NCET, and the Fundamental Research Funds for the Central Universities, and the Research Funds of Renmin University of China (No. 10XNJ002) (M.L.); NSERC of Canada, FQRNT of Quebec, and Canadian Institute of Advanced Research for partial support (H.G). We thank the HKU Computer Centre for providing computing facilities that were supported in part by the Hong Kong UGC Special Equipment Grant (SEG HKU09).

[1]T. Driscoll *et al.*, Appl. Phys. Lett. **95**, 043503 (2009).
[2]R. E. Simpson *et al.*, Nat. Nanotechnol. **6**, 501 (2011).
[3]E. Gerstner, Nat. Phys. **7**, 837 (2011).
[4]M. Valden, X. Lai, and D. W. Goodman, Science **281**, 1647 (1998).
[5]J. Muscat, V. Swamy, and N. M. Harrison, Phys. Rev. B **65**, 224112 (2002).
[6]E. Cho *et al.*, Phys. Rev. B **73**, 193202 (2006).
[7]Q. F. Xia *et al.*, Nanotechnology **22**, 254026 (2011).
[8]S. E. Savel'ev, A. S. Alexandrov, A. M. Bratkovsky, and R. S. Williams, Nanotechnology **22**, 254011 (2011).
[9]D. B. Strukov, G. S. Snider, D. R. Stewart, and R. S. Williams, Nature **453**, 80 (2008).
[10]L. O. Chua, IEEE Trans. Circuit Theory **18**, 507 (1971).
[11]S. R. Ovshinsky, Phys. Rev. Lett. **21**, 1450 (1968).
[12]J. P. Strachan, J. J. Yang, R. Munstermann *et al.*, Nanotechnology **20**, 485701 (2009).
[13]D. H. Kwon *et al.*, Nat. Nanotechnol. **5**, 148 (2010).
[14]K. Szot, W. Sperier, G. Bihlmayer, and R. Waser, Nature Mater. **5**, 312 (2006).
[15]K. Shibuya, R. Dittmann, S. B. Mi, and R. Waser, Adv. Mater. **22**, 411 (2010).
[16]D. S. Jeong, H. Schroeder, and R. Waser, Phys. Rev. B **79**, 195317 (2009).
[17]T. Prodromakis, B. P. Peh, C. Papavassiliou, and C. Toumazou, IEEE Trans. Electron Devices **58**, 3099 (2011).
[18]C. Yoshida, K. Tsunoda, H. Noshiro, and Y. Sugiyama, Appl. Phys. Lett. **91**, 223510 (2007).
[19]M. J. Rozenberg, I. H. Inoue, and M. J. Sanchez, Phys. Rev. Lett. **92**, 178302 (2004).
[20]B. Poumellec, P. J. Durham, and G. Y. Guo, J. Phys.: Condens. Matter **3**, 8195 (1991).
[21]Z. R. Zhang *et al.*, Phys. Rev. Lett. **99**, 126105 (2007).
[22]R. S. Williams, IEEE Spectrum **45**, 29 (2008).
[23]F. Pan, S. Yin, and V. Subramanian, IEEE Electron Device Lett. **32**, 949 (2011).
[24]M. Noman, W. K. Jiang, P. A. Salvador, M. Skowronski, and J. A. Bain, Appl. Phys. A **102**, 877 (2011).
[25]J. J. Yang *et al.*, Nanotechnology **20**, 215201 (2009).
[26]A. Asamitsu, Y. Tomioka, H. Kuwahara, and Y. Tokura, Nature **388**, 50 (1997).
[27]M. Simon, M. Nardone, V. G. Karpov, and I. V. Karpov, J. Appl. Phys. **108**, 064514 (2010).
[28]J. J. Yang *et al.*, Adv. Mater. **22**, 4034 (2010).
[29]R. Muenstermann, T. Menke, R. Dittmann, and R. Waser, Adv. Mater. **22**, 4819 (2010).
[30]R. W. Munn, J. Phys. C **8**, 2721 (1975).
[31]X. J. Liu *et al.*, Appl. Phys. Lett. **99**, 113518 (2011).

Downloaded 07 May 2013 to 147.8.230.100. This article is copyrighted as indicated in the abstract. Reuse of AIP content is subject to the terms at: http://jap.aip.org/about/rights_and_permissions

[32] C. Schindler, G. Staikov, and R. Waser, Appl. Phys. Lett. **94**, 072109 (2009).
[33] V. G. Karpov, Y. A. Kryukov, I. V. Karpov, and M. Mitra, Phys. Rev. B **78**, 052201 (2008).
[34] See www.nanoacademic.ca for more details of the Nanodcal package.
[35] J. Taylor, H. Guo, and J. Wang, Phys. Rev. B **63**, 245407 (2001); **63**, 121104 (2001).
[36] J. P. Perdew and Y. Wang, Phys. Rev. B **45**, 13244 (1992).
[37] L. Kleinman and D. M. Bylander, Phys. Rev. Lett. **48**, 1425 (1982).

Downloaded 07 May 2013 to 147.8.230.100. This article is copyrighted as indicated in the abstract. Reuse of AIP content is subject to the terms at: http://jap.aip.org/about/rights_and_permissions